Synthesis, Structural Characterisation and Nuclear Magnetic Resonance Study of $[Ru_6C(CO)_{15}(\mu_3\text{-}\eta^1:\eta^2:\eta^2\text{-}C_{16}H_{16}\text{-}\mu\text{-}O)]$: an Intermediate in the Formation of $[Ru_6C(CO)_{14}(\mu_3\text{-}\eta^2:\eta^2:\eta^2\text{-}C_{16}H_{16})]$†

Paul J. Dyson,[a] Brian F. G. Johnson,*[a] Caroline M. Martin,[a] David Reed,[a] Dario Braga*[b] and Fabrizia Grepioni[b]

[a] *Department of Chemistry, The University of Edinburgh, West Mains Road, Edinburgh EH9 3JJ, UK*
[b] *Dipartimento di Chimica 'G. Ciamician,' Università degli Studi di Bologna, Via Selmi 2, 40126 Bologna, Italy*

The complex $[Ru_6C(CO)_{15}(\mu_3\text{-}\eta^1:\eta^2:\eta^2\text{-}C_{16}H_{16}\text{-}\mu\text{-}O)]$ has been isolated and fully characterised in solution by ^1H NMR spectroscopy and in the solid state by single-crystal X-ray diffraction analysis. On heating it undergoes quantitative conversion to the carbido cluster, $[Ru_6C(CO)_{14}(\mu_3\text{-}\eta^2:\eta^2:\eta^2\text{-}C_{16}H_{16})]$, with the expulsion of CO_2, and on this basis may be considered as a key intermediate in the formation of the carbido cluster. This complex is a rare example of a molecular system containing both the carbido and oxo ligand, possibly derived from the cleavage of a carbonyl group, which are trapped within a metal-cluster framework. The isolation of this new cluster may be taken to indicate that the initial attack by a co-ordinated carbonyl group appears to take place on the co-ordinated organo moiety, thereby providing evidence for an intramolecular mechanism.

The initial discovery of $[Fe_5C(CO)_{15}]$[1] and the subsequent discovery of $[Ru_6C(CO)_{17}]$[2] led to a widespread interest in carbido clusters and precipitated studies into the origin of the carbido atom. Work with isotopically enriched ^{13}CO enabled workers to confirm that the source of the isolated C atom was a co-ordinated CO ligand and that the cluster unit brought about the disproportionation of carbon monoxide, $2CO \longrightarrow$ 'C' + CO_2.[3] The relevance that these discoveries bore on the activation of CO on metal surfaces was immediately recognised but the precise method by which the C–O bond cleavage occurs is still a matter of some debate. A single-crystal X-ray diffraction study of $[Fe_4H(CO)_{13}]^-$ revealed a molecular structure in which a butterfly arrangement of the four iron atoms supported a $\mu_4:\eta^2$-bonded CO ligand in which the C–O bond length was lengthened significantly.[4] This lent support to the view that the cluster unit activates the CO moiety by interaction of both the C and O simultaneously with several metal atoms. The significance of this observation was soon realised and compared with the formation of a carbide on the surface.[5] In all these experiments, the O atom appeared to be transferred to an adjacently bonded CO ligand by nucleophilic attack on the strongly electrophilic carbon. The dissociation of a bridging CO into carbido and oxo ligands is important in the metal-catalysed Fischer–Tropsch reaction. In 1992, Chisholm *et al.*[6] reported a tetratungsten cluster which provided the first example of a molecular system containing both the carbide and oxide ligands of a cleaved carbonyl. The cluster $[W_4(\mu_4\text{-}C)(O)(OPr^i)_{12}]$ is similar to that reported here and contains both a carbido ligand bonded to four tungsten atoms in a butterfly arrangement, and an oxo ligand bonded to two of the tungsten atoms. In a recent report, the reactivity of a CO molecule bridging metal atoms in these tungsten clusters has been compared to that of a CO molecule bridging metal atoms on a metal surface.[7] Both the CO bound to alkoxidotetratungsten $[W_4(OR)_{12}]$ clusters and the CO adsorbed on a sparsely covered Mo(110) surface react with dissociation to give carbido and oxo ligands bonded to neighbouring metal centres. In this paper we wish to report further studies on hexaruthenium-cluster systems which we believe shed further light on this intriguing chemistry.

Results and Discussion

We have recently observed that three compounds containing the [2.2]paracyclophane ligand, *viz.* $[Ru_3(CO)_9(\mu_3\text{-}\eta^2:\eta^2:\eta^2\text{-}C_{16}H_{16})]$ **1**, $[Ru_6C(CO)_{14}(\mu_3\text{-}\eta^2:\eta^2:\eta^2\text{-}C_{16}H_{16})]$ **3** and $[Ru_6C(CO)_{11}(\mu_3\text{-}\eta^2:\eta^2:\eta^2\text{-}C_{16}H_{16})(\eta^6\text{-}C_{16}H_{16})]$ **4**, may be obtained from the thermolysis of $[Ru_3(CO)_{12}]$ with [2.2]paracyclophane ($C_{16}H_{16}$) in heptane or octane.[8] An additional product has also been isolated from the same reaction, albeit in modest yield. This new cluster has been fully characterised in solution by ^1H NMR studies and in the solid state by single-crystal X-ray diffraction as $[Ru_6C(CO)_{15}(\mu_3\text{-}\eta^1:\eta^2:\eta^2\text{-}C_{16}H_{16}\text{-}\mu\text{-}O)]$ **2**. The IR spectrum shows CO stretches between 2085 and 1866 cm^{-1} which are typical of terminal and bridging carbonyl groups. The mass spectrum contains a parent peak at 1262 (calc. = 1263) which is followed by the sequential loss of fifteen CO groups. The ^1H NMR spectrum of **2** is rather complicated and will be described later, however, it is worth noting that this spectroscopic technique indicates the presence of two closely related isomers in solution, not revealed by IR spectroscopy which may be separated chromatographically.

In a separate experiment we have found that on heating $[Ru_3(CO)_9(\mu_3\text{-}\eta^2:\eta^2:\eta^2\text{-}C_{16}H_{16})]$ **1** with an equimolar quantity of $[Ru_3(CO)_{12}]$ both the open cluster **2** and the octahedral carbido species **3** are formed. Furthermore, the thermolysis of compound **2** in octane or its pyrolysis in a gas cell, yields cluster **3** and CO_2 almost quantitatively. Hence, it follows that **2** is an intermediate in the formation of **3**, merely requiring the loss of CO_2 and a rearrangement of the hexaruthenium polyhedron (see Scheme 1).

The molecular structure of **2** is illustrated in Fig. 1 together with the atomic labelling scheme; relevant structural parameters are listed in Table 1. The metal-atom core can be described as an open octahedron, the reference structure is that of $[Ru_6C(CO)_{17}]$ or of any face-capped derivative of this

† *Supplementary data available*: see Instructions for Authors, *J. Chem. Soc., Dalton Trans.*, 1995, Issue 1, pp. xxv–xxx.

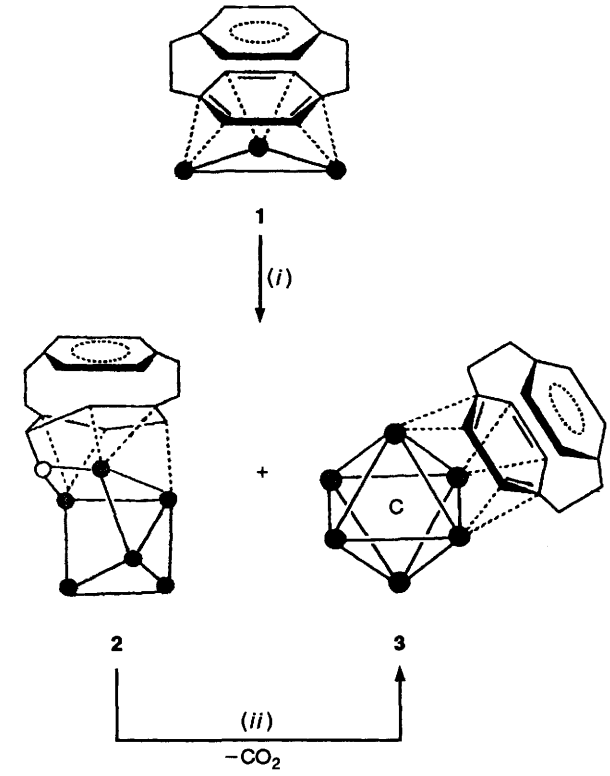

Scheme 1 Thermolysis of **1** with $[Ru_3(CO)_{12}]$. (*i*) Octane, $[Ru_3(CO)_{12}]$, heat; (*ii*) octane, heat or pyrolyse in gas cell

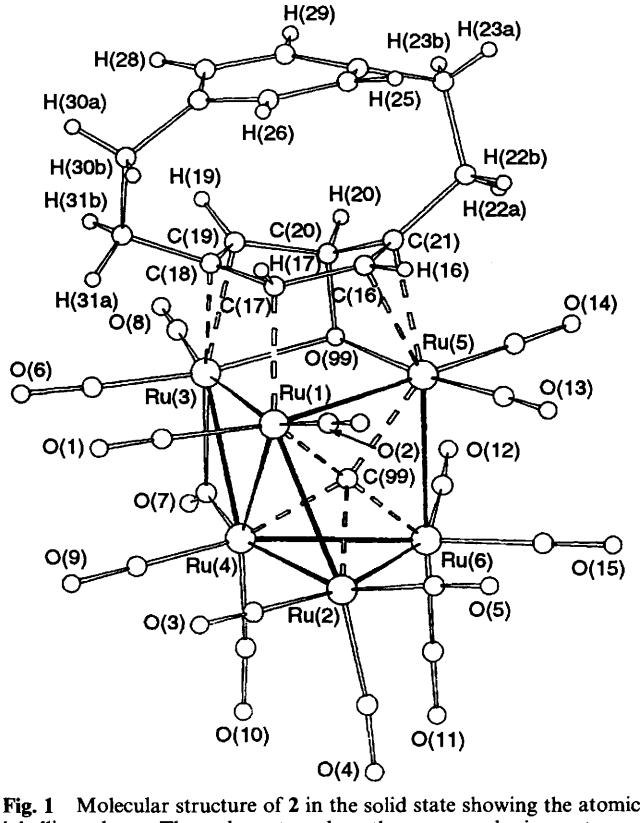

Fig. 1 Molecular structure of **2** in the solid state showing the atomic labelling scheme. The carbon atoms bear the same numbering system as their corresponding oxygen atoms

molecule, in particular **3**.[9] Three Ru–Ru edges are open with respect to the octahedral metal core. The interstitial carbido atom lies in the centre of the cavity formed by the ruthenium atoms 1, 2, 4, 5 and 6. The open edge between Ru(3) and Ru(5) is spanned by a bridging oxygen atom. There are a total of 15 CO ligands; Ru(2) and Ru(6) each carry three terminal CO ligands; the other basal atom Ru(4) carries two terminal COs and one bridging CO which asymmetrically spans the Ru(3)–Ru(4) edge. The three metal atoms which also interact with the cyclophane moiety carry two terminal CO ligands each, while Ru(3) is also involved in the aforementioned CO bridge. The interstitial carbido atom sits in the middle of a bridged-butterfly subsystem defined by Ru(1) and Ru(6) (wing-tip atoms) and Ru(2) and Ru(4) (hinge atoms), the wing-tips being bridged by Ru(5). The distances between the carbido atom and the wing-tip ruthenium atoms [1.94(3), 1.97(3) Å] are shorter than those from the bridging atom [Ru(5)–C(99) 2.04(2) Å] and from the hinge atoms [2.09(2) and 2.17(2) Å]; Ru(3) is at 3.11 Å.

The cyclophane ligand interacts with three metal atoms of the cluster. While the outer C_6 ring, although severely distorted, clearly shows the presence of a delocalised bonding pattern, the co-ordinated ring can be regarded as comprising of a 1,3-diene unit. The two C=C double bonds are located between C(17) and C(18) [1.38(3) Å] and C(16) and C(21) [1.34(3) Å]. The two unsaturated systems, however, do not have the same type of interaction with the cluster framework. The C(16)–C(21) bond establishes a 'conventional' π interaction by both C atoms being at a bonding distance from the Ru(5) atom [Ru(5)–C(16) 2.38(2), Ru(5)–C(21) 2.23(2) Å]. The second short C=C bond, instead of eclipsing a Ru atom, is *quasi*-parallel to the bond, with only one C atom C(17) interacting with Ru(1) [Ru(1)–C(17) 2.22(2) Å]. The fourth interaction is between C(19) and Ru(3) [2.20(2) Å], and C(18) also interacts with Ru(3) but at the longer distance of 2.60(2) Å. The bonded ring therefore contributes a

Table 1 Selected bond lengths (Å) and angles (°) for cluster **2**

Ru(1)–Ru(2)	2.868(3)	Ru(5)–C(16)	2.38(2)
Ru(1)–Ru(3)	2.913(3)	Ru(5)–C(20)	2.67(2)
Ru(1)–Ru(4)	2.817(3)	Ru(5)–C(21)	2.23(2)
Ru(1)–Ru(5)	2.847(3)	C(16)–C(17)	1.48(3)
Ru(2)–Ru(4)	2.707(3)	C(17)–C(18)	1.38(3)
Ru(2)–Ru(6)	2.864(3)	C(18)–C(19)	1.49(3)
Ru(3)–Ru(4)	2.782(3)	C(19)–C(20)	1.54(3)
Ru(4)–Ru(6)	2.933(3)	C(20)–C(21)	1.56(3)
Ru(5)–Ru(6)	2.846(3)	C(21)–C(16)	1.34(3)
Ru(1)–C(99)	1.94(3)	C(21)–C(22)	1.53(3)
Ru(2)–C(99)	2.17(2)	C(22)–C(23)	1.55(3)
Ru(4)–C(99)	2.09(2)	C(23)–C(24)	1.52(4)
Ru(5)–C(99)	2.04(2)	C(24)–C(25)	1.39(3)
Ru(6)–C(99)	1.97(3)	C(25)–C(26)	1.38(3)
Ru(3)–O(99)	2.14(2)	C(26)–C(27)	1.37(3)
Ru(5)–O(99)	2.06(2)	C(27)–C(28)	1.44(3)
O(99)–C(20)	1.40(3)	C(28)–C(29)	1.36(4)
Ru(1)–C(17)	2.22(2)	C(24)–C(29)	1.37(3)
Ru(3)–C(18)	2.60(2)	C(27)–C(30)	1.51(3)
Ru(3)–C(19)	2.20(2)	C(30)–C(31)	1.55(3)
Ru(3)–C(20)	2.70(2)	C(31)–C(18)	1.52(3)
C(21)–C(16)–C(17)	126(2)	C(23)–C(24)–C(25)	123(2)
C(18)–C(17)–C(16)	120(2)	C(23)–C(24)–C(29)	120(2)
C(17)–C(18)–C(19)	117(2)	C(25)–C(24)–C(29)	116(2)
C(17)–C(18)–C(31)	127(2)	C(24)–C(25)–C(26)	121(2)
C(19)–C(18)–C(31)	114(2)	C(25)–C(26)–C(27)	120(2)
C(18)–C(19)–C(20)	119(2)	C(26)–C(27)–C(28)	120(2)
C(19)–C(20)–C(21)	113(2)	C(26)–C(27)–C(30)	118(2)
C(16)–C(21)–C(22)	121(2)	C(28)–C(27)–C(30)	120(2)
C(20)–C(21)–C(16)	114(2)	C(27)–C(28)–C(29)	116(2)
C(20)–C(21)–C(22)	121(2)	C(28)–C(29)–C(24)	125(3)
C(21)–C(22)–C(23)	120(2)	C(27)–C(30)–C(31)	112(2)
C(22)–C(23)–C(24)	108(2)	C(18)–C(31)–C(30)	111(2)

mean Ru–C(O) (non-bridging)	1.90(3)
mean Ru–C(O) (bridging)	2.15(3)
C(7)–O(7) (bridging)	1.13(3)
mean C–O (non-bridging)	1.14(3)

total of five electrons. The distribution of bond lengths and angles is in agreement with the assignment of an sp^3 hybridisation to atom C(20) which forms a σ bond with the oxygen atom (see below). The other five atoms may each be considered to have an sp^2 hybridisation.

The bridging oxygen atom is pyramidal; the C–O distance of 1.40(3) Å is in agreement with a C–O single bond and the two Ru–O interactions are slightly different in length [Ru(3)–O(99) 2.14(2), Ru(5)–O(99) 2.06(2) Å] with an inner angle at the oxygen atom of 117.2(7)°. The oxygen atom is required to contribute three electrons to the cluster leaving one 'unused' lone pair, and the total electron count of the cluster is therefore 90. From Fig. 2 the oxygen atom appears to be deeply embedded within the ligand shell formed by the CO ligands and the cyclophane. It is clear that the lone pair resident on the oxygen atom occupies the 'niche' in the ligand envelope and is therefore available on the cluster surface for electrophilic attack and further reaction. It is also interesting to observe how the two CO ligands on both sides of the oxygen atom are repelled from the centre of the bridging system, similar to that observed with bridging hydrogen atoms.

The situation described is reminiscent of the bonding in $[Ru_3H(CO)_9(\mu_3\text{-}\eta^1:\eta^2:\eta^2\text{-}C_6H_7)]$ where the ligand lies nearly parallel to the metal triangle and contributes a total of five electrons to the cluster.[10] In this latter case, however, the $CH\text{–}CH_2\text{–}CH$ portion of the ligand spans the H(bridged) Ru–Ru bond whereas in the present case the sp^3 carbon atom interacts with the bridging oxygen atom.

The ^1H NMR spectrum of **2** is shown in Fig. 3. It comprises several multiplets which, for convenience, are labelled A–Q. Three protons give rise to the group of signals labelled D–F, two to signal B and two to signal N/P. The spectrum is consistent with a [2.2]paracyclophane group asymmetrically bound to the cluster. Signal assignment has been achieved from a series of homonuclear decoupling and NOE experiments, using the premise that the signal L corresponds to H(20), which is bound to the sp^3 carbon atom, and that signals M–Q arise from the protons associated with the 'remote' non-bonded aromatic ring.

Decoupling of signal L resulted in the loss of a 6.2 Hz

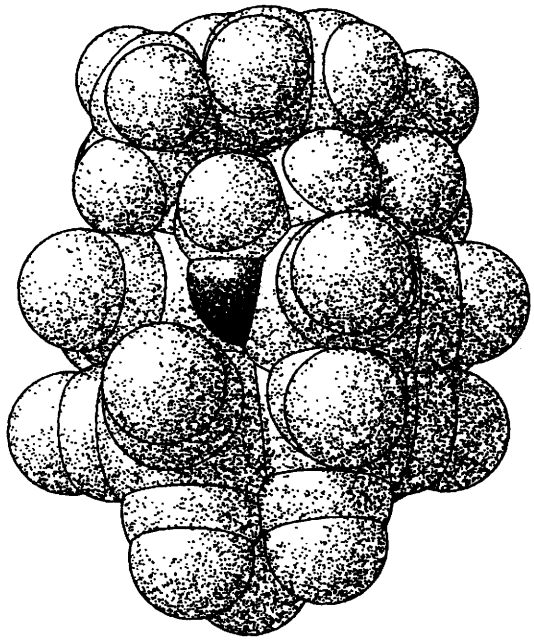

Fig. 2 Space-filling representation of the structure of **2** showing the oxygen atom embedded in the ligand envelope

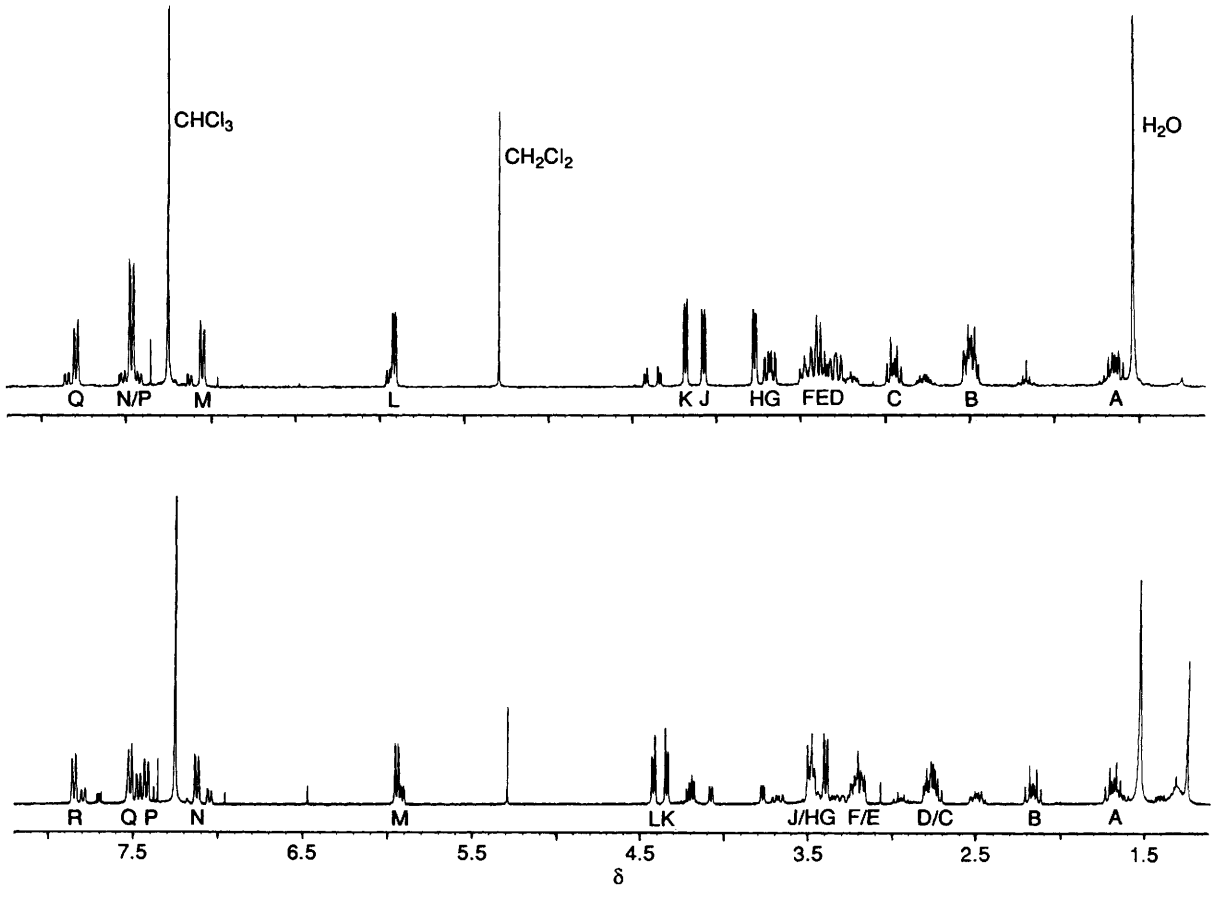

Fig. 3 ^1H NMR spectrum of **2** (top) and **2a** (bottom)

coupling from signal J, and a 2.1 Hz coupling from signal H. Hence J arises from H(19), with H(16) producing signal H; K therefore arises from H(17), this has been confirmed from a decoupling experiment which links it to H(16). The signal labelled N/P has been shown to arise from two different protons by observing the effects of decoupling at both M and Q respectively, with decoupling at either site M or site Q causing one of the N/P pair to lose a 7.9 Hz coupling and the other to lose a 1.6 Hz coupling. Hence M and Q do not couple with each other, and are *para* to each other on the aromatic ring.

The results of a series of NOE experiments performed on **2** are summarised in Table 2, and show that interactions between protons on the two 'aromatic' ring systems may be detected and they further permit the complete assignment of the spectrum shown in Fig. 3. Thus, saturation of signal H [H(16)] results in enhancements of A, K and N/P, allowing them to be assigned to protons H(22a), H(17) and H(25), respectively. The saturation of K [H(17)] enhances signals G, H and M, confirming G as arising from H(31a) and M from H(26). It follows that the assignments given in Table 3 may be derived with confidence. In all cases, the NOE results are consistent with the proposed assignment.

The initial ^{1}H NMR spectrum also showed evidence for the presence of a second isomeric form of **2**, *viz.* **2a**. Both isomers are produced in the initial thermolysis, and are of very similar physical appearance, they may just be separated by chromatography. Spectroscopic analysis (IR and mass spectrometry) reveal that **2a** is very similar to **2** differing only in the interaction of the $C_{16}H_{16}O$ moiety with the Ru_6C cluster unit.

Thus, the ^{1}H NMR spectrum of this minor isomer **2a** (Fig. 3) is similar to that of **2**. The signal M is consistent with a proton attached to an oxygen-bearing carbon (*cf.* signal L from isomer **2**) and the signals N–R are consistent with those from a 'remote' aromatic ring of a cyclophane bound to a metal cluster. The primary differences between the ^{1}H NMR spectra of the two isomers lay in the δ values of the protons associated with the bound aromatic ring. The assignments for the relevant protons in **2a** were determined *via* decoupling of signal M, using a similar numbering scheme for **2a** as for **2**.

Mechanistic Proposals.—As already outlined, it has been proposed that carbido atoms may be introduced into metal-cluster compounds by the thermally induced cleavage of a co-ordinated carbon monoxide ligand. Carbon dioxide is usually detected as a by-product from these reactions, indicating that the disproportionation of two carbonyl groups has occurred. It has been suggested that C–O bond cleavage occurs more readily if the carbonyl ligand is co-ordinated in a dihapto manner,[6,11] and may even be an essential step in any reaction sequence. In order that this bonding mode for a CO ligand may be adopted, the initial loss of CO ligands is required in order to bring about a co-ordinatively unsaturated cluster unit thereby opening up active sites for CO cleavage. The multihapto co-ordination of a carbonyl ligand leads to a considerable elongation and weakening of the C–O bond (evidenced by C–O stretching frequencies), therefore making cleavage relatively easy. Additionally, this co-ordination mode increases the nucleophilicity of the carbonyl oxygen, enabling attack at the electrophilic carbon of a terminal carbonyl necessary for the formation of CO_2. One might, therefore, expect to form an ester-type intermediate which then breaks down into CO_2 and the observed cluster carbide, which is similar to a mechanism proposed by Deeming.[12]

Clusters containing η^2-bonded carbonyl ligands are relatively rare but a cluster intermediate containing such a dihapto carbonyl ligand has been isolated and shown to be involved in the formation of a hexaruthenium carbido cluster.[13] In this example the thermolysis of $[Ru_3(CO)_{12}]$ in heptane–mesitylene yields the complex $[Ru_6C(CO)_{14}(\eta^6\text{-}C_6H_3Me_3)]$, together with the two compounds $[Ru_6(\eta^2\text{-}\mu_4\text{-}CO)_2(CO)_{13}(\eta^6\text{-}C_6H_3Me_3)]$ and $[Ru_6H(\eta^2\text{-}\mu_4\text{-}CO)(CO)_{13}(\mu\text{-}\eta^1:\eta^6\text{-}C_6H_3Me_2CH_2)]$. Furthermore, the thermolysis of $[Ru_6(\eta^2\text{-}\mu_4\text{-}CO)_2(CO)_{13}(\eta^6\text{-}C_6H_3Me_3)]$ in mesitylene, results in its conversion to $[Ru_6C(CO)_{14}(\eta^6\text{-}C_6H_3Me_3)]$ and $[Ru_6H(\eta^2\text{-}\mu_4\text{-}$

Table 2 Results of a series of NOE experiments performed on **2**, the percentage enhancements are indicated

	Irradiation site													
	A	B	C	D	E	F	G	H	J	K	L	M	N/P	Q
A								4						
B	10.5			2			10.5		2		2			
C				18			4					5		
D			19											
E														2.5
F	1													
G			3							2				
H	7.5									11			2	
J											11			
K			2				6	13				4		
L									11					7.5
M			8							4				
N/P				3				6	3.5			5		5
Q											4			

Table 3 Assignments of the ^{1}H NMR spectrum signals with regard to the H positions in the solid-state structure

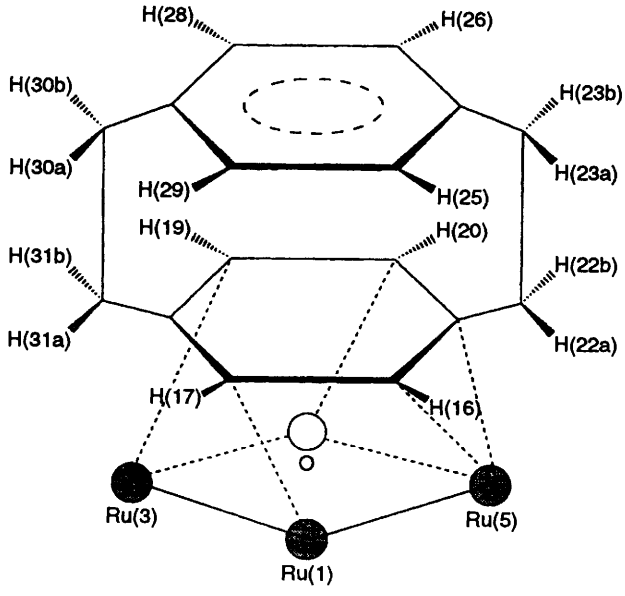

H position	^{1}H signal	δ	Multiplicity; *J* (H–H) Hz
H(16)	H	3.78	d of d; 5.8, 2.1
H(17)	K	4.18	d of d; 5.8, 1.6
H(19)	J	4.08	d of d; 6.2, 1.6
H(20)	L	5.91	d of d; 6.2, 2.1
H(22a)	A	1.64	d of d of d; 13.8, 9.7, 7.8
H(22b)	B	2.4–2.55	Overlapping multiplet
H(23a)	F	3.2–3.5	Overlapping multiplet
H(23b)	E	3.2–3.5	Overlapping multiplet
H(25)	N/P	7.46	d of d; 7.9, 1.6
H(26)	M	7.05	d of d; 7.9, 1.6
H(28)	N/P	7.46	d of d; 7.9, 1.6
H(29)	Q	7.79	d of d; 7.9, 1.6
H(30a)	C	2.95	d of t; 13.6, 8.6
H(30b)	D	3.2–3.5	Overlapping multiplet
H(31a)	G	3.68	d of d of d; 14.0, 8.8, 1.6
H(31b)	B	2.4–2.55	Overlapping multiplet

$CO)(CO)_{13}(\mu\text{-}\eta^1:\eta^6\text{-}C_6H_3Me_2CH_2)]$ in equal amounts, together with CO_2. Here it would appear that the mechanism of carbide formation is intermolecular and involves the cleavage of an η^2-CO ligand of $[Ru_6(\eta^2\text{-}\mu_4\text{-}CO)_2(CO)_{13}(\eta^6\text{-}C_6H_3Me_3)]$ *via* nucleophilic attack of its oxygen on a terminal CO carbon of a second cluster molecule. Elimination of CO_2 from this intermediate generates the carbide co-ordinated to the first cluster, which can undergo rearrangement to encapsulate this newly formed carbido atom and so produces the complex $[Ru_6C(CO)_{14}(\eta^6\text{-}C_6H_3Me_3)]$.

We believe that cluster **2** represents the next stage in the reaction mechanism after the C–O bond cleavage of a dihapto carbonyl ligand has occurred but before the oxygen atom has been expelled from the cluster as CO_2. The proposed mechanism differs slightly from that described above in that the nucleophilic oxygen attacks a ring carbon of the cyclophane moiety within the same molecule, instead of the carbon atom of a terminal CO on a second molecule. This is easy to envisage since co-ordination to a metal centre induces electrophilicity into the cyclophane-ring carbons making them more susceptible to attack by the carbonyl oxygen. As a result, the weak C–O bond undergoes cleavage producing the observed intermediate $[Ru_6C(CO)_{15}(\mu_3\text{-}\eta^1:\eta^2:\eta^2\text{-}C_{16}H_{16}\text{-}\mu\text{-}O)]$ **2**. Since the cluster has a particularly open geometric framework, an intramolecular mechanism for the conversion of **2** to **3** can be envisaged in which CO_2 is generated and rapidly expelled from the cluster core and is detected by IR spectroscopy when the process is carried out in a gas cell. The cluster now contains 14 CO ligands (the number present in cluster **3**) and rearrangement of the metal-atom network, with the simultaneous movement of the carbide and ligands, to produce the 86-electron octahedral cluster **3** may readily take place. The stability of the octahedrally encapsulated carbido atom in this system, together with the production of CO_2 undoubtedly contribute to the driving force for the C–O cleavage process described.

Conclusion

It would appear that the oxygen atom of an activated CO may be transferred to a co-ordinated organo group and provides an alternative view of the generation of oxygen-containing organic substrates. The transfer of the same oxygen to a CO leading to the reduction of the organic substrate is also of some interest. This work in addition emphasises the danger of a simplistic view of CO cleavage and again leads to the conclusion that in cluster chemistry at least, such reactivities may be *intra-* rather than *inter*-molecular. Significantly, the crystal structure provides direct evidence for this phenomenon.

Experimental

All reactions were carried out with the exclusion of air using freshly distilled solvents under an atmosphere of dry nitrogen. Subsequent work-up of products was achieved without precautions to exclude air with standard laboratory grade solvents. Infrared spectra were recorded on a Perkin-Elmer 1710 Series FTIR in CH_2Cl_2 using NaCl cells. Positive fast-atom-bombardment mass spectra were obtained using a Kratos MS50TC spectrometer, with CsI as calibrant. All NMR spectra were recorded on a Bruker AM360 spectrometer. The conditions for homonuclear NOE and decoupling experiments have been described elsewhere.[14] All the ^1H and ^{13}C NMR spectra described herein were recorded in $CDCl_3$ solutions, and referenced to tetramethylsilane at 0 ppm. Products were separated chromatographically by using either a column fitted with nitrogen pressurisation containing silica 60 mesh or by thin layer on plates supplied by Merck coated with a 0.25 mm layer of Kieselgel 60 F254. [2.2]Paracyclophane was purchased from Fluka Chemicals and used without further purification.

Thermolysis of $[Ru_3(CO)_{12}]$ *with* [2.2]*Paracyclophane*.—A suspension of $[Ru_3(CO)_{12}]$ (500 mg) in octane (30 cm^3) containing a large excess of [2.2]paracyclophane (200 mg) was heated to reflux for 2 h. The reaction was monitored by spot TLC and IR spectroscopy, both of which indicated the complete consumption of starting material after this time. The solvent was removed *in vacuo*, and the products separated by column chromatography, using a solution of dichloromethane–hexane (3:7) as eluent. In order of elution, the products were characterised spectroscopically as $[Ru_3(CO)_9(\mu_3\text{-}\eta^2:\eta^2:\eta^2\text{-}C_{16}H_{16})]$ **1** (yellow, 15%), $[Ru_6C(CO)_{14}(\mu_3\text{-}\eta^2:\eta^2:\eta^2\text{-}C_{16}H_{16})]$ **3** (red, 20%), $[Ru_6C(CO)_{15}(\mu_3\text{-}\eta^1:\eta^2:\eta^2\text{-}C_{16}H_{16}\text{-}\mu\text{-}O)]$ **2** (purple, 5%) (Found: C, 30.05; H, 1.35. Calc. for $C_{32}H_{16}O_{16}Ru_6$: C, 30.45; H, 1.25%) and $[Ru_6C(CO)_{11}(\mu_3\text{-}\eta^2:\eta^2:\eta^2\text{-}C_{16}H_{16})(\eta^6\text{-}C_{16}H_{16})]$ **4** (brown, 3%). A longer reaction time of 4 h afforded greater yields of **3** and **4**, whereas if the thermolysis reaction was carried out in heptane for 3 h, compound **1** was the major product (30%), with an enhanced yield of **2** (10%). Further purification of **2** by thin-layer chromatography using the same eluent resulted in two purple bands which only just resolved, the main one being **2** and the minor lower band **2a**.

Spectroscopic data for $[Ru_6C(CO)_{15}(\mu_3\text{-}\eta^1:\eta^2:\eta^2\text{-}C_{16}H_{16}\text{-}\mu\text{-}O)]$ **2**: $\tilde{\nu}_{CO}/cm^{-1}$ (CH_2Cl_2) 2084m, 2053s, 2037vs, 2016m, 2008m, 1067w and 1866w; *m/z* 1262 (calc. = 1263). NMR: ^1H, δ 7.79 (d of d, 1 H, *J* 7.9, 1.6), 7.46 (d of d, 2 H, *J* 7.9, 1.6), 7.05 (d of d, 1 H, *J* 7.9, 1.6), 5.91 (d of d, 1 H, *J* 6.2, 2.1), 4.18 (d of d, 1 H, *J* 5.8, 1.6), 4.08 (d of d, 1 H, *J* 6.2, 1.6), 3.78 (d of d, 1 H, *J* 5.8, 2.1), 3.68 (d of d of d, 1 H, *J* 14.0, 8.8, 1.6), 3.2–3.5 (overlapping multiplets, 3 H), 2.95 [d of t, 1 H, *J* 13.6 (d), 8.6], 2.4–2.55 (overlapping multiplets, 2 H) and 1.64 (d of d of d, 1 H, *J* 13.8, 9.7, 7.8 Hz); ^{13}C ([2.2]paracyclophane resonances only, the assignment of signals as CH, CH_2, CH_3 or quaternary, q, was achieved using a DEPT pulse sequence), δ 138.2 (q), 136.9 (q), 133.8 (CH), 133.6 (CH), 133.4 (CH), 130.1 (CH), 109.2 (q), 88.3 (CH), 74.4 (CH), 65.1 (q), 47.4 (CH), 39.8 (CH_2), 35.8 (CH_2), 34.6 (CH_2), 34.3 (CH_2) and 21.6 (CH).

2a. ^1H NMR: δ 7.84 (d of d, 1 H, *J* 7.9, 1.6), 7.52 (d of d, 1 H, *J* 7.8, 1.8), 7.42 (d of d, 1 H, *J* 7.9, 1.6), 7.12 (d of d, 1 H, *J* 7.9, 1.8), 5.94 (d of d, 1 H, *J* 6.9, 1.8), 4.42 (d of d, 1 H, *J* 5.9, 1.8), 4.35 (d of d, 1 H, *J* 5.9, 1.7), *ca.* 3.5 (overlapping signals, 2 H), 3.40 (d of d, 1 H, *J* 6.9, 1.7), *ca.* 3.2 (overlapping multiplets, 2 H), *ca.* 2.75 (overlapping multiplets, 2 H), 2.16 [d of t, 1 H, *J* 114.88 (d), 9.5] and 1.69 [d of t, 1 H, *J* 13.9 (d), 9.2 Hz].

Table 4 Crystal data and details of measurements for cluster **2**

Formula	$C_{32}H_{16}O_{16}Ru_6{\cdot}CH_2Cl_2$
M	1 347.8
T/K	150
System	Orthorhombic
Space group	$Pca2_1$
a/Å	18.270(4)
b/Å	10.432(6)
c/Å	19.825(6)
U/Å^3	3781(2)
Z	4
F(000)	2568
λ(Mo-Kα)/Å	0.710 69
μ(Mo-Kα)/mm^{-1}	2.368
θ range/°	2.8–22.6
Octants explored (*h*, *k*, *l*)	0–19, 0–11, 0–21
Measured reflections	2849
Unique observed reflections	2581
Unique observed reflections [$I_o > 2\sigma(I_o)$]	2162
No. of refined parameters	334
Goodness of fit on F^2	1.052
Final *R* indices [$I > \sigma(I)$] R_1 (on *F*), wR_2 (on F^2)	0.0543, 0.1047
Final *R* indices (all data) R_1 (on *F*), wR_2 (on F^2)	0.0736, 0.1168

Table 5 Atomic coordinates ($\times 10^4$) for cluster **2**

Atom	*x*	*y*	*z*	Atom	*x*	*y*	*z*
Ru(1)	1 418(1)	6 669(2)	4 146(1)	O(11)	2 533(11)	10 742(19)	1 900(9)
Ru(2)	2 663(1)	7 648(2)	3 432(1)	C(12)	944(16)	10 894(29)	3 051(15)
Ru(3)	47(1)	7 026(2)	3 421(1)	O(12)	403(10)	11 438(20)	2 960(9)
Ru(4)	1 383(1)	7 319(2)	2 767(1)	C(13)	1 849(14)	9 636(24)	4 975(13)
Ru(5)	1 053(1)	9 264(2)	4 432(1)	O(13)	2 367(10)	9 759(18)	5 321(11)
Ru(6)	1 797(1)	9 897(2)	3 215(1)	C(14)	759(14)	10 937(28)	4 552(14)
C(99)	1 561(13)	8 281(24)	3 676(12)	O(14)	569(10)	12 004(18)	4 623(9)
O(99)	95(8)	8 829(15)	3 931(7)	C(15)	2 327(13)	11 108(24)	3 728(13)
C(1)	1 454(13)	4 826(25)	3 970(11)	O(15)	2 669(9)	11 832(17)	4 056(9)
O(1)	1 461(9)	3 830(17)	3 833(9)	C(16)	603(12)	7 817(22)	5 260(12)
C(2)	2 132(13)	6 511(23)	4 864(12)	C(17)	596(12)	6 511(22)	4 964(11)
O(2)	2 554(9)	6 410(16)	5 281(9)	C(18)	−17(12)	6 085(23)	4 632(12)
C(3)	2 963(13)	5 895(26)	3 422(15)	C(19)	−538(12)	7 075(20)	4 388(11)
O(3)	3 128(8)	4 849(17)	3 411(11)	C(20)	−342(12)	8 501(22)	4 481(12)
C(4)	3 327(16)	8 243(28)	2 751(15)	C(21)	133(11)	8 760(19)	5 118(10)
O(4)	3 690(11)	8 504(23)	2 316(10)	C(22)	−115(13)	9 697(23)	5 665(12)
C(5)	3 310(12)	8 201(21)	4 124(12)	C(23)	−804(14)	9 398(25)	6 094(13)
O(5)	3 699(10)	8 553(17)	4 513(11)	C(24)	−896(13)	7 949(23)	6 126(12)
C(6)	−45(13)	5 351(24)	3 116(13)	C(25)	−393(13)	7 150(24)	6 442(13)
O(6)	−120(9)	4 301(16)	2 943(9)	C(26)	−326(11)	5 884(22)	6 259(11)
C(7)	416(14)	7 714(25)	2 370(13)	C(27)	−789(14)	5 376(24)	5 787(12)
O(7)	81(11)	8 034(22)	1 924(10)	C(28)	−1 412(13)	6 112(24)	5 562(12)
C(8)	−862(14)	7 468(25)	3 037(13)	C(29)	1 427(14)	7 361(25)	5 753(12)
O(8)	−1 383(9)	7 741(17)	2 807(9)	C(30)	−508(13)	4 285(25)	5 358(12)
C(9)	1 491(15)	5 639(28)	2 507(14)	C(31)	−324(14)	4 731(23)	4 632(12)
O(9)	1 595(10)	4 537(18)	2 373(9)	C(32)	3 085(20)	3 924(35)	1 432(18)
C(10)	1 835(15)	7 830(27)	1 939(15)	Cl(1)	3 409(5)	3 374(9)	659(4)
O(10)	2 101(11)	8 034(20)	1 458(8)	Cl(2)	3 400(5)	5 345(10)	1 697(5)
C(11)	2 279(14)	10 412(25)	2 388(14)				

Thermolysis of $[Ru_3(CO)_9(\mu_3\text{-}\eta^2\text{:}\eta^2\text{:}\eta^2\text{-}C_{16}H_{16})]$ **1** *with* $[Ru_3(CO)_{12}]$.—The compounds $[Ru_3(CO)_9(\mu_3\text{-}\eta^2\text{:}\eta^2\text{:}\eta^2\text{-}C_{16}H_{16})]$ **1** (50 mg) and $[Ru_3(CO)_{12}]$ (42 mg, 1 mol equiv.) were dissolved in octane (30 cm^3) and the reaction mixture heated to reflux for 3 h, during which time the colour of the solution darkened from orange to deep red. Monitoring the reaction by spot TLC indicated that 3 h was an optimum time in which the balance between the remaining starting material and the decomposition material was achieved. The solvent was removed *in vacuo* and the residue purified by TLC using a solution of dichloromethane–hexane (3:7) as eluent. Apart from the remaining starting material **1** (12%), two bands, one red and one purple, were isolated and characterised spectroscopically as $[Ru_6C(CO)_{15}(\mu_3\text{-}\eta^1\text{:}\eta^2\text{:}\eta^2\text{-}C_{16}H_{16}\text{-}\mu\text{-}O)]$ **2** (8%) and $[Ru_6C(CO)_{14}(\mu_3\text{-}\eta^2\text{:}\eta^2\text{:}\eta^2\text{-}C_{16}H_{16})]$ **3** (26%), respectively.

Thermolysis of $[Ru_6C(CO)_{15}(\mu_3\text{-}\eta^1\text{:}\eta^2\text{:}\eta^2\text{-}C_{16}H_{16}\text{-}\mu\text{-}O)]$ **2** *in Octane.*—The compound $[Ru_6C(CO)_{15}(\mu_3\text{-}\eta^1\text{:}\eta^2\text{:}\eta^2\text{-}C_{16}H_{16}\text{-}\mu\text{-}O)]$ **2** (10 mg) was heated to reflux in octane (20 cm^3) for 3 h. During this time the reaction mixture was monitored spectroscopically (IR) which indicated that all the starting material had been consumed. The solvent was removed under reduced pressure and the product extracted by TLC using a solution of dichloromethane–hexane (3:7) as eluent. The major red band was collected and characterised by spectroscopy as $[Ru_6C(CO)_{14}(\mu_3\text{-}\eta^2\text{:}\eta^2\text{:}\eta^2\text{-}C_{16}H_{16})]$ **3** (90%).

Solid-state Pyrolysis of $[Ru_6C(CO)_{15}(\mu_3\text{-}\eta^1\text{:}\eta^2\text{:}\eta^2\text{-}C_{16}H_{16}\text{-}\mu\text{-}O)]$ **2**.—The compound $[Ru_6C(CO)_{15}(\mu_3\text{-}\eta^1\text{:}\eta^2\text{:}\eta^2\text{-}C_{16}H_{16}\text{-}\mu\text{-}O)]$ **2** (10 mg) was placed in the bulb in the floor of an IR gas cell (NaCl windows, 10 cm path length). The cell was evacuated, sealed, then placed in the spectrometer and a background recorded. The bulb containing the compound was heated to *ca.* 200 °C for 2 min and a second IR spectrum recorded. The IR spectrum clearly showed that CO_2 had been evolved. The remaining solid was dissolved in dichloromethane and characterised as $[Ru_6C(CO)_{14}(\mu_3\text{-}\eta^2\text{:}\eta^2\text{:}\eta^2\text{-}C_{16}H_{16})]$ **3**.

Structural Characterisation.—Diffraction data for compound **2** was collected on a Stoë Stadi-4 four-circle diffractometer equipped with a graphite monochromator (Mo-Kα radiation, λ = 0.710 73 Å). An Oxford Cryosystems low-temperature device was used for the determination.[15] Details of the crystal data, data collection and structure refinement are summarised in Table 4. The structure was solved by direct methods,[16] and a series of Fourier-difference maps were used to locate all light atoms except the H atoms. These atoms were placed in geometrically calculated positions. Considering the peculiarities of the structure, our main concern was with a precise definition of the atomic species corresponding to the interstitial and to the bridging atoms. Four independent refinements were carried out by attributing in all possible combinations the atomic scattering factors of carbon and oxygen. The test in which the interstitial atom was treated as carbon and the bridging atom as oxygen gave not only the lowest agreement index but also the most sensible combination of isotropic thermal parameters. Fractional atomic coordinates for **2** are listed in Table 5.

Finally, it is worth mentioning that **2** also crystallises in another form without dichloromethane solvate. The cell parameters are as follows: space group triclinic, a = 9.504(5), b = 12.918(6), c = 17.667(14) Å, α = 109.76(5), β = 102.44(6), γ = 80.81(4)° and U = 1984(2) Å^3. Unfortunately the quality of the crystal data collected on this latter crystal is poor and does not justify a deeper discussion. However, it is important to stress that the key structural features of this species are identical to those discussed above.

All calculations were performed using SHELXL 93[17] and the molecular graphics were carried out using SCHAKAL 93.[18]

Additional material available from the Cambridge Crystallographic Data Centre comprises H-atom coordinates, anisotropic thermal parameters and remaining bond lengths and angles.

Acknowledgements

We thank the University of Edinburgh, the EPRSC and ICI (Wilton) (C. M. M.) for financial assistance. Financial support

by MURST (Italy) is also acknowledged (D. B. and F. G.) and NATO is thanked for a travel grant (D. B., F. G. and B. F. G. J.).

References

1 E. H. Braye, L. F. Dahl, W. Hübel and D. L. Wampler, *J. Am. Chem. Soc.*, 1962, **84**, 4633.
2 B. F. G. Johnson, R. D. Johnston and J. Lewis, *J. Chem. Soc., Chem. Commun.*, 1967, 1057.
3 S. Martinengo, B. T. Heaton, R. J. Goodfellow and P. Chini, *J. Chem. Soc., Chem. Commun.*, 1977, 39; I. A. Oxton, S. F. A. Kettle, P. F. Jackson, B. F. G. Johnson and J. Lewis, *J. Chem. Soc., Chem. Commun.*, 1979, 687.
4 M. Manssero, M. Sansoni and G. Longoni, *J. Chem. Soc., Chem. Commun.*, 1976, 919.
5 V. Ponec, *Catal. Rev. Sci. Eng.*, 1978, **18**, 151; W. A. Herrmann, *Angew. Chem., Int. Ed. Engl.*, 1982, **21**, 117.
6 M. H. Chisholm, C. E. Hammond, V. J. Johnston, W. E. Streib and J. C. Huffman, *J. Am. Chem. Soc.*, 1992, **114**, 7056.
7 B. C. Gates, *Angew. Chem., Int. Ed. Engl.*, 1993, **32**, 228.
8 P. J. Dyson, B. F. G. Johnson, C. M. Martin, A. J. Blake, D. Braga, F. Grepioni and E. Parisini, *Organometallics*, 1994, **13**, 2113.
9 D. Braga, F. Grepioni, E. Parisini, P. J. Dyson, A. J. Blake and B. F. G. Johnson, *J. Chem. Soc., Dalton Trans.*, 1993, 2951.
10 B. F. G. Johnson, J. Lewis, M. Martinelli, A. H. Wright, D. Braga and F. Grepioni, *J. Chem. Soc., Chem. Commun.*, 1990, 364; D. Braga, F. Grepioni, E. Parisini, B. F. G. Johnson, C. M. Martin, J. G. M. Nairn, J. Lewis and M. Martinelli, *J. Chem. Soc., Dalton Trans.*, 1993, 1891.
11 E. L. Muetteries, *Bull. Soc. Chim. Belg.*, 1975, **85**, 959; 1976, **86**, 451.
12 A. J. Deeming, in *Transition Metal Clusters*, ed. B. F. G. Johnson, Wiley, New York, 1980, p. 415.
13 C. E. Anson, P. J. Bailey, G. Conole, B. F. G. Johnson, J. Lewis, M. McPartlin and H. R. Powell, *J. Chem. Soc., Chem. Commun.*, 1989, 442; P. J. Bailey, M. J. Duer, B. F. G. Johnson, J. Lewis, G. Conole, M. McPartlin, H. R. Powell and C. E. Anson, *J. Organomet. Chem.*, 1990, **383**, 441.
14 C. R. McIntyre, D. Reed, I. H. Sadler and T. J. Simpson, *J. Chem. Soc., Perkin Trans. 1*, 1989, 1987.
15 J. Cosier and A. M. Glazer, *J. Appl. Crystallogr.*, 1986, **19**, 105.
16 G. M. Sheldrick, SHELXS 86, Program for crystal structure solution, *Acta Crystallogr., Sect. A*, 1990, **46**, 467.
17 G. M. Sheldrick, SHELXL 93, Program for crystal structure refinement, University of Göttingen, 1993.
18 E. Keller, SCHAKAL 93, Graphical representation of molecular models, University of Freiburg, 1993.

Received 31*st May* 1995; *Paper* 5/03474D